Supplemental Material for Curvature-dependence of the liquid-vapor surface tension beyond the Tolman approximation

Nicolas Bruot and Frédéric Caupin
Institut Lumière Matière, UMR5306 Université Claude Bernard Lyon 1-CNRS, Université de Lyon and Institut Universitaire de France, 69622 Villeurbanne cedex, France

This note provides additional information on the experiments and the analysis presented in the Letter, and presents an analysis of *n*-heptane and water nucleation data to complement the ethanol data. It also discusses the uncertainties and approximations to support our conclusions. When not specified, the notations and legends in this document are the same as in the main text.

CONTENTS

I. MATERIALS AND METHODS

We have performed acoustic cavitation in n-heptane (Sigma Aldrich, puriss. p.a., $\geq$ 99%) and ethanol (VWR Prolabo Chemicals, 99.98% v/v), using a hemispherical piezoelectric transducer to focus 1 MHz sound bursts (a few cycles long) in a small region of the liquid far from any wall[1]. Ramping the excitation voltage of the transducer, the cavitation probability increases from 0 to 1. The "cavitation threshold" corresponds to a 50% cavitation probability during a burst. In a previous study[2], the pressure at the focus was estimated indirectly by studying the effect of the static pressure in the liquid on the cavitation threshold. Here, we have measured the density of the fluid at the focus directly with a fiber-optic probe hydrophone[3], which is sensitive to the modulation of the refractive index by the sound wave. To convert the density into a pressure, we used an equation of state for the liquid at positive pressure, and extrapolated it down to about -30 MPa. More details will be given elsewhere.

II. COMPARISON BETWEEN THE STATIC PRESSURE AND FOPH METHODS

Fig. 1(a) and S1(a) show pressures at the cavitation threshold slightly more negative with the FOPH than the previously reported values. Here we give an explanation for the discrepancy.

The static pressure method in Ref. 2 was based on the dependence of the transducer voltage at the cavitation threshold on the positive static pressure applied to the liquid. A linear extrapolation gave an indirect estimate of the negative cavitation pressure. However, nonlinearities lead to extrapolated pressures less negative than the real ones[4]. The new experiments with a FOPH give direct access to the density of the liquid at the cavitation threshold. The only remaining assumption resides here in the conversion of the density into a pressure, that requires to extrapolate to negative pressure an equation of state measured at positive pressure. In the case of water, we have previously measured the equation of state at negative pressure and proven that this assumption is valid[5]. It is reasonable to assume that the extrapolation would also be valid for heptane and ethanol, thus yielding to FOPH points that are more accurate than the points from the static pressure method.

III. STUDY OF n-HEPTANE AND WATER

The analysis carried in the Letter on ethanol can be extended to other liquids. Figures S1, S2, S3, S4 below show results for n-heptane and water.

IV. FORMULA OF THE MODIFIED CNTS

This sections gives the formula we have used to calculate the CNT_1 and CNT_2 parameters, and the critical volumes from the nucleation theorem.

A. CNT_1

In the CNT_1, Eq. (8) is written at the critical radius, $R_\mathrm{s} = R_\mathrm{s}^*$. R_s^* is trivially deduced from the Laplace equation as a function of the energy barrier $\Delta\Omega$, and ΔP, that are known from the experiments:

$$R_\mathrm{s}^* = \left(\frac{3\Delta\Omega}{2\pi\Delta p}\right)^{1/3} . \tag{S1}$$

Since Eq. (3) with $R_\mathrm{s} = R_\mathrm{s}^*$ links $\sigma_\mathrm{s}(R_\mathrm{s}^*)$ to $\Delta\Omega$ and R_s^*, we obtain the following expression for the Tolman length:

$$\delta_\infty = \frac{\sigma_\infty}{\Delta P}\left[1 - \left(\frac{3\Delta\Omega}{16\pi\sigma_\infty^3}\right)^{1/3}\right] . \tag{S2}$$

Compared to CNT_0, the critical equimolar radius now depends on δ_∞. The derivation is done in Ref. 6 and gives

$$R_\mathrm{e}^* = \frac{2\sigma_\infty}{\Delta P} - \delta_\infty . \tag{S3}$$

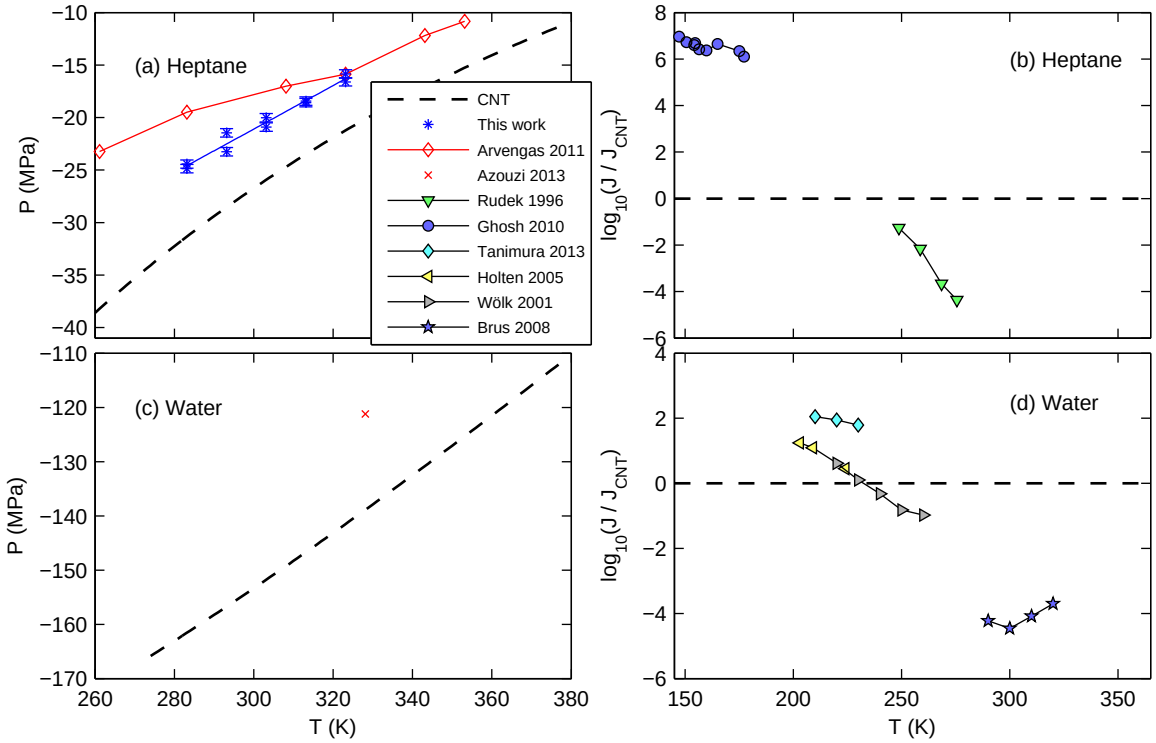

FIG. S1. Same as Fig. 1 in the Letter, but for (a,b) heptane and (c,d) water. The point in (c) corresponds to the cavitation pressure measurement in a water inclusion in a quartz crystal[14].

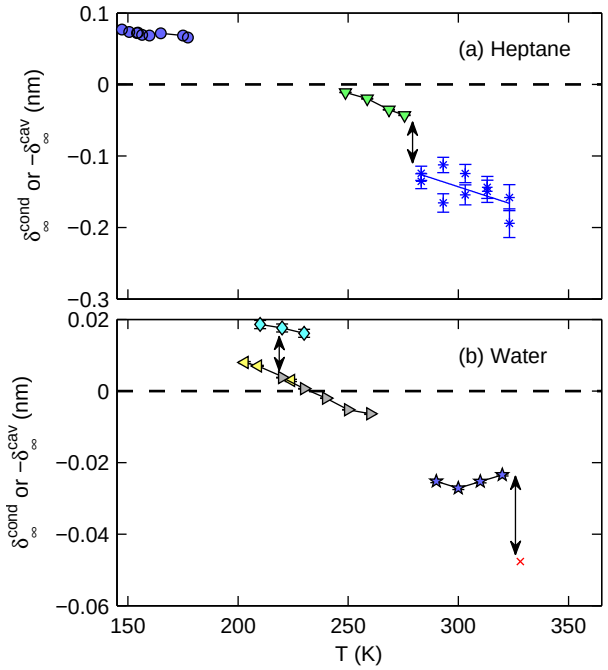

FIG. S2. Same as Fig. 2, but for (a) heptane and (b) water.

B. CNT_2

Eqs. (2), (7) and (9) form a system of equations that can be solved for δ_∞ and $\delta_\infty^2+\alpha$. The relevant solutions are

$$\begin{cases} \delta_\infty &= -\dfrac{R_\mathrm{s}^*}{2}(1-\sqrt{\Delta}) \\ \delta_\infty^2+\alpha &= (R_\mathrm{s}^*)^2\left(\dfrac{2\sigma_\infty}{R_\mathrm{s}^*\Delta P}-\sqrt{\Delta}\right), \end{cases} \tag{S4}$$

where

$$\Delta = 1-\frac{4R_\mathrm{e}^*}{R_\mathrm{s}^*}+\frac{8\sigma_\infty}{R_\mathrm{s}^*\Delta P}\,. \tag{S5}$$

Here, R_e^* is obtained in the experiments from the nucleation theorem and R_s^* is given by Eq. (S1).

C. Choice for the kinetic prefactor

1. Cavitation

The CNT_0 and its variants CNT_1 and CNT_2 rely on the choice of an expression for the kinetic prefactor J_0.

For cavitation, we chose $J_0V\tau = 10^{19}$, where V is the volume where the acoustic wave is focalized, and τ the duration of an acoustic burst. The value is taken from our previous study in water[1]. The actual value of $J_0V\tau$ in the present experiments might differ from the 10^{19} value. However, a change by a factor 10 in this constant only leads to a shift of the experimental points by about 0.015 nm for the CNT_1's δ_∞ and 0.5 nm^3 for V_e^* (for both heptane and ethanol). This is much smaller than the statistical deviations seen by repeating cavitation pressure measurements at the same temperature several times.

2. Condensation

For condensation, the nucleation rates are calculated from the supersaturation $S = P_\mathrm{v}/P_\mathrm{sat}(T)$, where P_v is the pressure of the metastable vapor, and $P_\mathrm{sat}(T)$ is the equilibrium vapor pressure for a flat interface. Treating the vapor as a perfect gas, and the liquid as an incompressible phase leads to:

$$\Delta P = \frac{kT\ln S}{v_\mathrm{l}}\,, \tag{S6}$$

where k is the Boltzmann constant and v_l the volume per molecule in the liquid. (Including gas non-idealities has been shown to have little effect on the nucleation rates for n-nonane[7].) For the kinetic prefactor, we used

$$J_0 = \sqrt{\frac{2\sigma_\infty}{\pi m_\mathrm{l}}}v_\mathrm{l}\,S^2\left(\frac{P_\mathrm{sat}(T)}{kT}\right)^2, \tag{S7}$$

with m_l the mass of a molecule. The actual value of J_0 is still being debated. In particular, a "$1/S$ correction" is sometimes added to Eq. (S7)[6]. This, again, only leads to insignificant changes in the quantities explored in this study. For instance, the typical shifts from the data in[8] are: 2 orders of magnitude for $J_\mathrm{exp}/J_\mathrm{CNT}$, 0.1 nm^3 for V_e^*, 0.02 nm for the CNT_1's δ_∞, and 2×10^{-4} nm and 0.015 nm^2 for the CNT_2's δ_∞ and $\delta_\infty^2+\alpha$.

D. Derivation of the critical volumes from the nucleation theorem

Critical volumes are obtained from the nucleation theorem Eq. (5). When writing Eq. (6) and converting Δn^* into a volume, two consecutive approximations are made. First, we assume that the density at the center of the nucleus is the density of the homogeneous phase, ρ_L or ρ_V. This allows us to link the critical volume to the excess number of molecules by:

$$V_\mathrm{e}^* = \frac{n_\mathrm{e}^*}{\rho_\mathrm{L}} = \frac{\Delta n^*}{\rho_\mathrm{L}-\rho_\mathrm{V}} \quad \text{for droplets} \tag{S8}$$

$$= \frac{n_\mathrm{e}^*}{\rho_\mathrm{V}} = -\frac{\rho_\mathrm{V}}{\rho_\mathrm{L}-\rho_\mathrm{V}}\Delta n^* \quad \text{for bubbles,} \tag{S9}$$

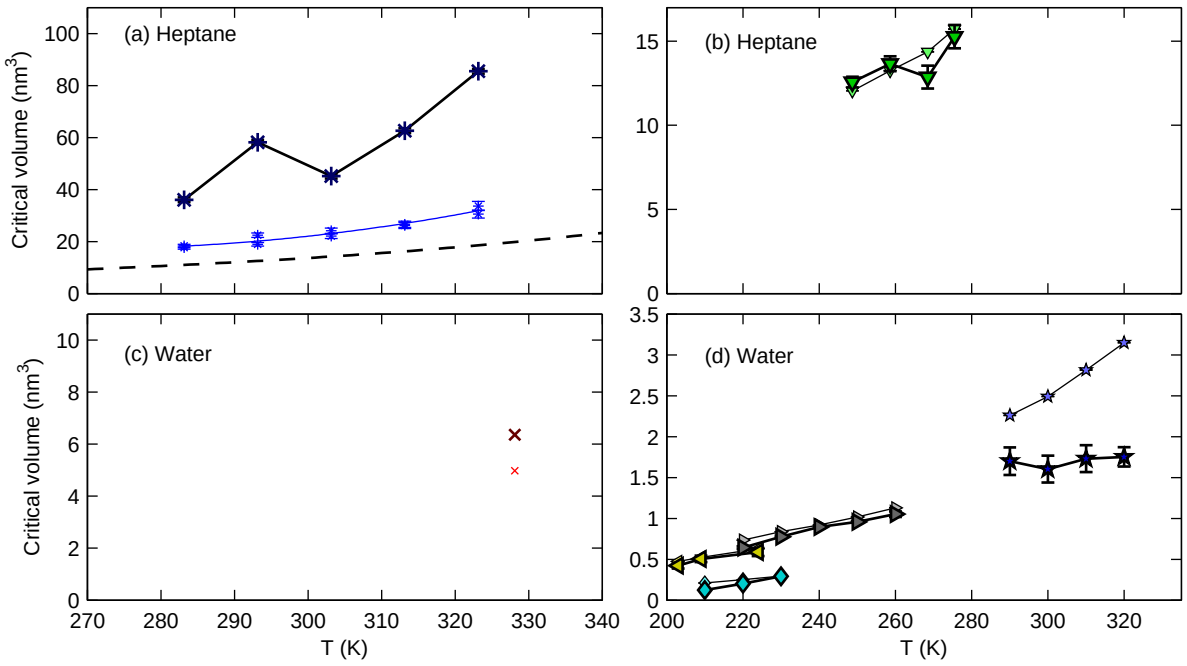

FIG. S3. Same as Fig. 3, but for (a,b) heptane and (c,d) water.

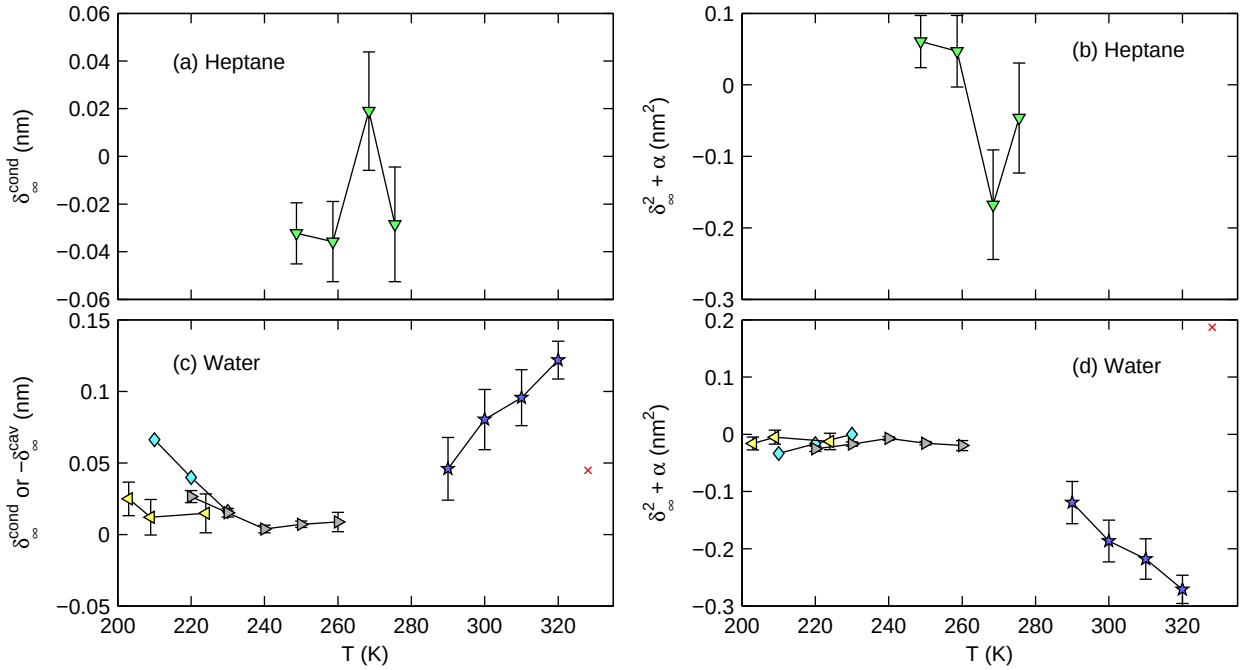

FIG. S4. Same as Fig. 4, but for (a,b) heptane and (c,d) water.

where n_e^* is the number of molecules in the nucleus. The second approximation we make is that $\rho_L \gg \rho_V$, which is easily satisfied: for the data analyzed in the Letter and here, the maximal value of ρ_V/ρ_L is 0.68×10^{-3} for condensation and 1.1×10^{-3} for the FOPH experiments. The critical volume then simply becomes

$$V_e^* = \frac{|\Delta n^*|}{\rho_L}, \tag{S10}$$

for droplets and bubbles.

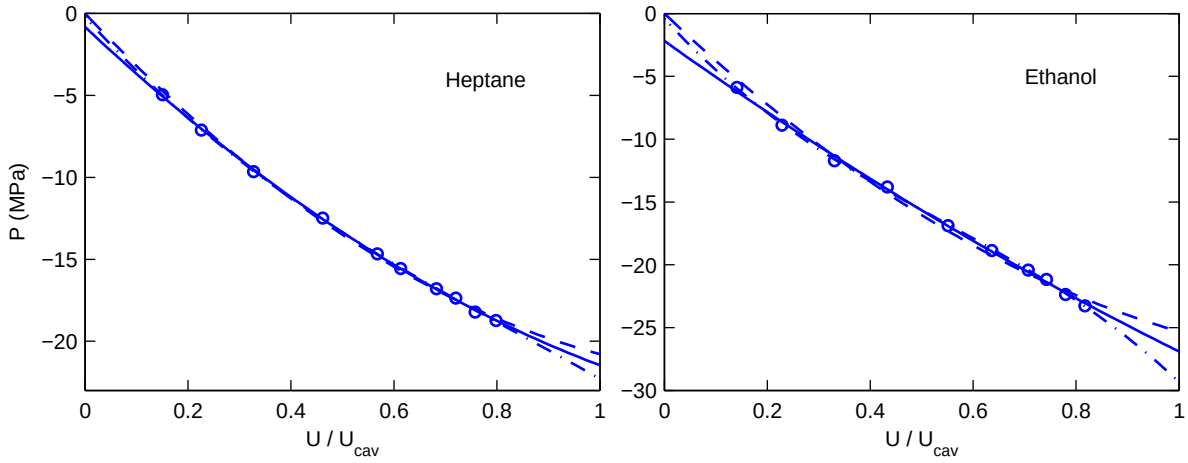

FIG. S5. Pressure depending on the amplitude of the voltage on the piezo-electric transducer for $T = 293$ K. The markers represent the measurements and the lines correspond to the different polynomials used to extrapolate the curve up to $U = U_{\rm cav}$: P_1 (dashed line), P_2 (solid line) and P_3 (dash-dotted line).

The two approximations above lead to an underestimate of the critical volumes[9,10]. Correcting for these would therefore make the discrepancy between the real critical volumes and the CNT_1's volumes that we highlight in the main text stronger.

V. EFFECT OF THE EXTRAPOLATION OF THE VOLTAGE TO PRESSURE RELATION (CAVITATION EXPERIMENTS)

A large part of the uncertainties in our experiments do not come from statistical error bars. To measure the cavitation pressures and the critical volumes in the fiber-optic probe hydrophone experiments, pressures are measured for different amplitudes of the sound wave created by a piezo-electric transducer. The amplitude is controlled by the amplitude of the oscillatory voltage U applied to the transducer (see Ref. 3 for details on the setup). Unfortunately, the voltage cannot be increased up to the value for which there would be 50 % chance to cavitate as it would damage the end facet of the fiber. To obtain the pressure $P_{\rm cav}$ at the voltage $U_{\rm cav}$, the pressure is measured for several values of U below about $0.8U_{\rm cav}$, and we fit the data with some function to extrapolate the pressures to $P_{\rm cav}$. We have tried several functions for the extrapolation, and three of them gave sufficiently small residuals:

$$P_1(U) = a_2U^2 + a_1U\,, \tag{S11}$$

$$P_2(U) = b_2U^2 + b_1U + b_0\,, \tag{S12}$$

and

$$P_3(U) = c_3U^3 + c_2U^2 + c_1U + c_0\,, \tag{S13}$$

where the a_i, b_i and c_i are the fitting coefficients. We show the three extrapolations for a given temperature in heptane and ethanol in Fig. S5. On this plot, $P_{\rm cav}$ can simply be read for $U = U_{\rm cav}$. To calculate the critical volumes from the nucleation theorem within the framework of CNT_1, Eq. (6) is rewritten in terms of a derivative $\partial P/\partial U$ of the pressure with the voltage, so that the critical volumes are related to the slope of $P(U)$ at $U_{\rm cav}$. Since we could not find any strong argument to determine which extrapolation is the best, we display in Figs. S6, S7 and S8 the quantities obtained with the three polynomials. The graphs of the main text (and their equivalents for heptane and water in Figs. S1, S2, S3 and S4) use polynomial P_2 as its residuals were slightly better than for the other functions and because it often lies between the values computed with P_1 and P_3. The choice of the function for the extrapolation can lead to significant changes of the various quantities plotted, especially the critical volumes. However, no matter what function is used, there is no master curve emerging in Fig. S7 (for heptane), and it appears very unlikely from Fig. S8 that the real critical volumes from the nucleation theorem could match the volumes from the CNT_1.

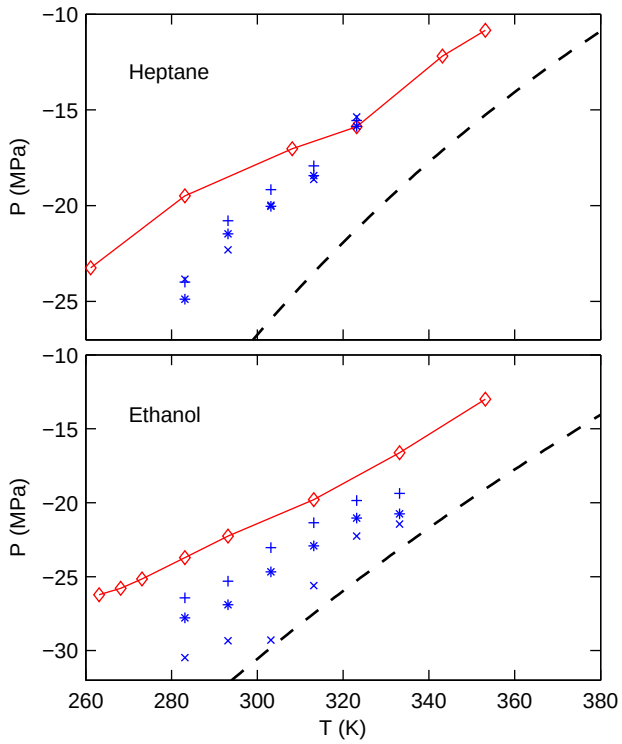

FIG. S6. Same as in Figs. 1 and S1 for one of the two FOPH series of measurements, but showing the results from the three functions P_1 (+ markers), P_2 (∗ markers) and P_3 (× markers).

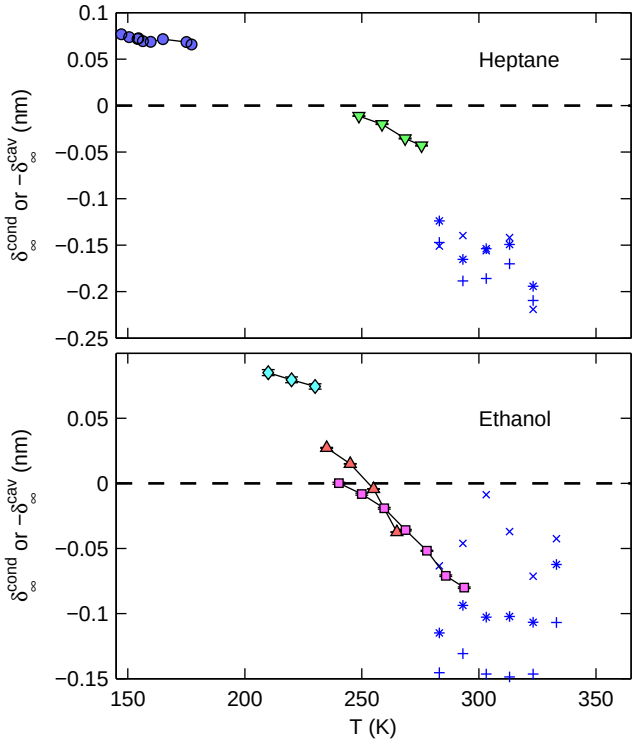

FIG. S7. Same as in Figs. 2 and S2 for one of the two FOPH series of measurements, but showing the results from the three functions P_1 (+ markers), P_2 (∗ markers) and P_3 (× markers).

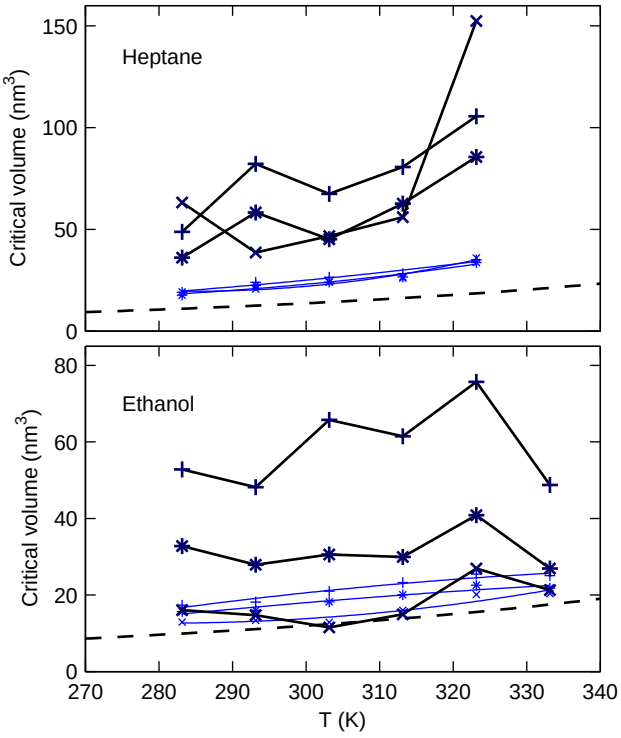

FIG. S8. Same as in Figs. 3 and S3, but showing the results from the three functions P_1 (+ markers), P_2 ($*$ markers) and P_3 ($\times$ markers).

VI. CNT_2 FOR CAVITATION

Cavitation data have been omitted in the CNT_2 analysis. The reason is that increasing the order also increases the error bars, and the errors induced by the $P(U)$ extrapolation (see above) lead to a large uncertainty in δ_∞ and $\delta_\infty^2 + \alpha$. Moreover, the values of the cavitation pressures and of the critical volumes are such that the solving of the second order polynomial to obtain the solutions in Eq. (S4) sometimes gives no real roots. Fig. S9 shows the cavitation analysis for the points that do have a solution, along with the condensation experiments. The systematic error induced by the choice of the $P(U)$ relation is typically of the order of the range of the y axis of the graphs for both δ_∞ and $\delta_\infty^2 + \alpha$.

VII. ESTIMATE OF THE STATISTICAL ERROR BARS

Whenever it was possible, we have put statistical error bars on the quantities δ_∞ and V_e^* from CNT_1, V_e^* from the NT, and δ_∞ and $\delta_\infty^2 + \alpha$ from the CNT_2. This section describes how they were calculated.

A. Fiber-optic probe hydrophone experiments

In the fiber-optic probe hydrophone (FOPH) experiments, the error bars in $\delta_\infty^{\mathrm{cav}}$ have been estimated on repeated experiments at a single temperature, $T = 293$ K. Between two cavitation pressure measurements, the fiber was removed and repositioned at the acoustic focal point. The results were dispersed with a standard deviation of 0.4 MPa, which we took as the error bar for all temperatures. To complement this statistical error, we also display, in the Letter and here, the FOPH measurements in heptane and ethanol for two series of temperatures (for each liquid). When switching to a new series, the fiber was cleaved to renew its end facet, which leads to an additional uncertainty in the measurements.

The critical volumes from the nucleation theorem V_e^* rely on a nonlinear fit of the probability to cavitate $\Sigma(U)$, with one of the parameters, ξ, representing the "width" of the $\Sigma(U)$ curve that has an "S" shape[2]. The error bar on ξ has been estimated for each liquid for a single temperature. Assuming that the experiment gave a set of points

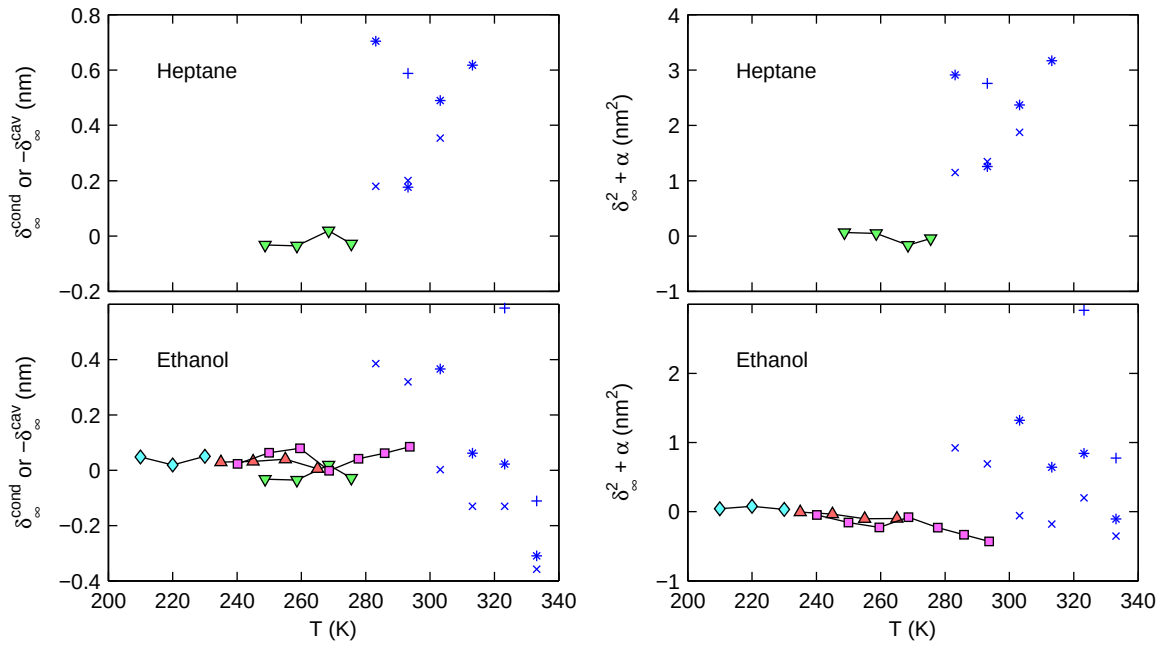

FIG. S9. Same as Figs. 4 and S4, but including the cavitation points with polynomial P_1 (+ markers), P_2 ($*$ markers) and P_3 ($\times$ markers).

$\{(U_{\rm exp}, \Sigma_{\rm exp})_i\}$, we have generated numerically several sets $\{(U_{\rm exp}, \Sigma_{\rm num})_i\}$ and fitted an S-curve on each of them, thus providing us with a standard error on ξ. The generation of a given point $(U_{\rm exp}, \Sigma_{\rm num})$ is done by taking for $\Sigma_{\rm num}$ a random value corresponding to the average of N values $\sigma_j \in \{0, 1\}$ with a probability of obtaining 1 equals to $\Sigma_{\rm exp}$.

B. Condensation experiments

The condensation data typically correspond to measurements of the nucleation rate J for different values of the supersaturation S, and of the temperature T. For a given temperature, the $S(J)$ curve is expected to be a portion of a line, and such a fit is indeed performed to obtain the critical volume $V_{\rm e}^*$. We extract two statistical errors from that fit:

- The standard error on the slope.
- A standard error on the average nucleation rate for the given temperature. When plotting the $S(J)$ fit function together with the experimental points, these are dispersed around the fit function. Assuming that there is an error in the J measurements, but that S is known precisely, this allows to estimate an overall statistical error in a single J measurement, ΔJ_0, from the deviation of the experimental J to the fit function.

These made possible the calculation of standard errors on the following quantities:

- The first error above is used to get the statistical error on $V_{\rm e}^*$ (from nucleation theorem).
- Since we used, for a given temperature, the average value (over all S) of J as an input in the δ_∞ and $V_{\rm e}^*$ formulas, the standard errors on these quantities simply derive from the standard error $\Delta J = \Delta J_0/\sqrt{N}$, with N the number of points for the fit.
- The δ_∞ and $\delta_\infty^2 + \alpha$ quantities both depend on the two parameters J and $V_{\rm e}^*$. We have noted that in most of the cases the error due to J in δ_∞ and $\delta_\infty^2 + \alpha$ is at least 10 times smaller than the error due to $V_{\rm e}^*$. We have therefore only included the standard error due to the critical volumes in δ_∞ and $\delta_\infty^2 + \alpha$.

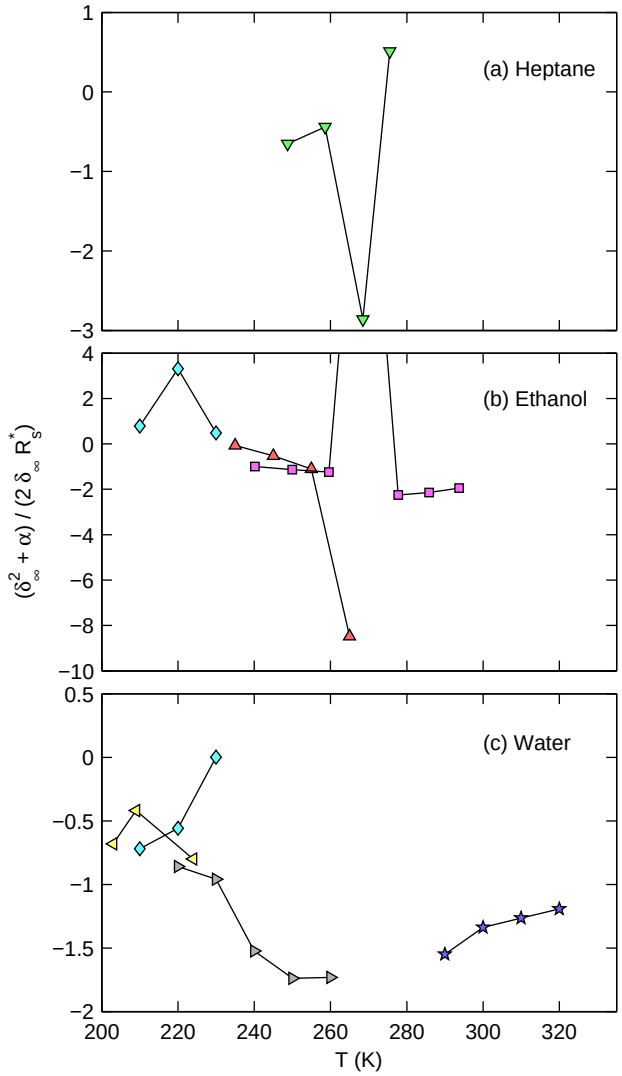

FIG. S10. Ratio between the second order term $(\delta_\infty^2 + \alpha)/(R_s^*)^2$ and the first order term $2\delta_\infty/R_s^*$. The point out of the graph for ethanol is at a height $(\delta_\infty^2 + \alpha)/(2\delta_\infty R_s^*) = 269$.

VIII. SECOND ORDER APPROXIMATION FOR THE SURFACE TENSION σ_s

A. Validity

Eq. (9) is derived by Taylor expanding and integrating the Gibbs-Tolman-Koenig-Buff (GTKB) equation (Eq. (26) in Ref. 11) to second order in $1/R_s^*$, by neglecting terms such as $\delta_\infty^3/(R_s^*)^3$ and $\alpha^2/(R_s^*)^4$. For each pair of values $(\delta_\infty, \delta_\infty^2 + \alpha)$ from the experiments, we have compared the value of σ_s from Eq. (9) with the full numerical integration of the GTKB equation. For the 34 points used to plot Figs. 4 and S4, the maximum relative error is 3.7 %, and 29 points give an error of less than 1 %, which makes Eq. (9) an excellent approximation for realistic ranges of parameters for condensation.

B. Comparison of the two terms in the σ_s expansion of the CNT_2

With the beginning of the use of models including a second order related to the rigidity of the interface, some debate emerged about the relative amplitudes of the two terms $2\delta_\infty/R_s^*$ and $(\delta_\infty^2 + \alpha)/(R_s^*)^2$. In simulations, models that include the second term only, or that include the two terms[12,13] have been tested. For the experiments, their ratio,

extracted from the condensation measurements, is shown in Fig. S10. Overall, we found that the two quantities are often of the same order of magnitude. Sometimes, the ratio takes values much larger than 1, but this only happens when δ_∞ is very close to 0, so that these points may have large error bars, because of the error in the δ_∞ values. Therefore, we expect that a model of a surface tension varying as $\sigma_\infty/\sigma_\mathrm{s} = 1 + C/(R_\mathrm{s}^*)^2$, with C a constant, would display inconsistencies similar to those found with the CNT_1 model.

IX. FITTED CNT_2 PARAMETERS FOR ETHANOL

Considering the condensation data only, we obtained an overall agreement of all the data in the sense that the points are closer to master curves for $\delta_\infty(T)$ and $(\delta_\infty^2 + \alpha)(T)$ in the CNT_2 than what was found for δ_∞ in the CNT_1. The best results are obtained for ethanol. We have fitted in this case these functions by simple expressions that can be used as empirical functions, namely a constant δ_∞ and a linear $\delta_\infty^2 + \alpha$:

$$\delta_\infty^2 + \alpha = A(T - T_\mathrm{ref}) + B\,. \tag{S14}$$

With $T_\mathrm{ref} = 298.15$ K, the fit parameters are $\delta_\infty = 0.04095$ nm, $A = -0.005460$ nm^2/K and $B = -0.3352$ nm^2.

[1] E. Herbert, S. Balibar, and F. Caupin, Cavitation pressure in water, *Phys. Rev. E* **74**, 041603 (2006).
[2] A. Arvengas, E. Herbert, S. Cersoy, K. Davitt, and F. Caupin, Cavitation in heavy water and other liquids, *J. Phys. Chem. B* **115**, 14240 (2011).
[3] A. Arvengas, K. Davitt, and F. Caupin, Fiber optic probe hydrophone for the study of acoustic cavitation in water, *Rev. Sci. Instrum.* **82**, 034904 (2011).
[4] C. Appert, C. Tenaud, X. Chavanne, S. Balibar, F. Caupin, and D. d'Humières, Nonlinear effects and shock formation in the focusing of a spherical acoustic wave, *Eur. Phys. J. B* **35**, 531 (2003).
[5] K. Davitt, E. Rolley, F. Caupin, A. Arvengas, and S. Balibar, Equation of state of water under negative pressure, *J. Chem. Phys.* **133**, 174507 (2010).
[6] V. Holten, D. G. Labetski, and M. E. H. van Dongen, Homogeneous nucleation of water between 200 and 240 K: New wave tube data and estimation of the Tolman length, *J. Chem. Phys.* **123**, 104505 (2005).
[7] J. A. Fisk and J. L. Katz, Condensation of supersaturated vapors. X. Pressure and nonideal gas effects, *J. Chem. Phys.* **104**, 8649 (1996).
[8] S. Tanimura, H. Pathak, and B. E. Wyslouzil, Binary nucleation rates for ethanol/water mixtures in supersonic Laval nozzles: Analyses by the first and second nucleation theorems, *J. Chem. Phys.* **139**, 174311 (2013).
[9] D. W. Oxtoby, Nucleation of first-order phase transitions, *Acc. Chem. Res.* **31**, 91 (1998).
[10] D. Kashchiev, Thermodynamically consistent description of the work to form a nucleus of any size, *J. Chem. Phys.* **118**, 1837 (2003).
[11] A. Tröster, M. Oettel, B. Block, Virnau, and K. Binder, Numerical approaches to determine the interface tension of curved interfaces from free energy calculations, *J. Chem. Phys.* **136**, 064709 (2012).
[12] B. J. Block, S. K. Das, M. Oettel, Virnau, and K. Binder, Curvature dependence of surface free energy of liquid drops and bubbles: A simulation study, *J. Chem. Phys.* **133**, 154702 (2010).
[13] V. G. Baidakov and K. S. Bobrov, Spontaneous cavitation in a Lennard-Jones liquid at negative pressures, *J. Chem. Phys.* **140**, 184506 (2014).
[14] M. E. M. Azouzi, C. Ramboz, J.-F. Lenain, and F. Caupin, A coherent picture of water at extreme negative pressure, *Nature Phys.* **9**, 38 (2013).